



Enhanced Role of Transition Metal Ion Catalysis During In-Cloud Oxidation of SO₂

Eliza Harris *et al.*

Science **340**, 727 (2013);

DOI: 10.1126/science.1230911

This copy is for your personal, non-commercial use only.

If you wish to distribute this article to others, you can order high-quality copies for your colleagues, clients, or customers by [clicking here](#).

Permission to republish or repurpose articles or portions of articles can be obtained by following the guidelines [here](#).

The following resources related to this article are available online at www.sciencemag.org (this information is current as of May 9, 2013):

Updated information and services, including high-resolution figures, can be found in the online version of this article at:

<http://www.sciencemag.org/content/340/6133/727.full.html>

Supporting Online Material can be found at:

<http://www.sciencemag.org/content/suppl/2013/05/08/340.6133.727.DC1.html>

This article **cites 83 articles**, 2 of which can be accessed free:

<http://www.sciencemag.org/content/340/6133/727.full.html#ref-list-1>

This article appears in the following **subject collections**:

Atmospheric Science

<http://www.sciencemag.org/cgi/collection/atmos>

Enhanced Role of Transition Metal Ion Catalysis During In-Cloud Oxidation of SO₂

Eliza Harris,^{1*†} Bärbel Sinha,^{1,2*} Dominik van Pinxteren,³ Andreas Tilgner,³ Khandeh Wadinga Fomba,³ Johannes Schneider,¹ Anja Roth,¹ Thomas Gnauk,³ Benjamin Fahlbusch,³ Stephan Mertes,³ Taehyoung Lee,⁴ Jeffrey Collett,⁴ Stephen Foley,^{5‡} Stephan Borrmann,^{1,6} Peter Hoppe,¹ Hartmut Herrmann³

Global sulfate production plays a key role in aerosol radiative forcing; more than half of this production occurs in clouds. We found that sulfur dioxide oxidation catalyzed by natural transition metal ions is the dominant in-cloud oxidation pathway. The pathway was observed to occur primarily on coarse mineral dust, so the sulfate produced will have a short lifetime and little direct or indirect climatic effect. Taking this into account will lead to large changes in estimates of the magnitude and spatial distribution of aerosol forcing. Therefore, this oxidation pathway—which is currently included in only one of the 12 major global climate models—will have a significant impact on assessments of current and future climate.

The size distribution and properties of atmospheric aerosol particles play a key role in the climate system by affecting how aerosols scatter radiation and modify the brightness and lifetime of clouds (1, 2). The magnitude of aerosol radiative forcing is the largest uncertainty in current climate assessments (3). Processing of particles in clouds changes both their size and hygroscopicity, and is therefore critical in determining the magnitude of aerosol radiative forcing. Sulfate addition to particles, through both in situ oxidation of SO₂ and direct uptake of H₂SO₄ gas and ultrafine particulate by cloud droplets, is the most important in-cloud mass production mechanism (4, 5) (table S1). A detailed understanding of the in-cloud sulfur cycle is therefore critical for accurate estimation of the current and future sulfate distribution and its impact on the climate through aerosol radiative forcing (6). The Hill Cap Cloud Thuringia (HCCT-2010) campaign, a Lagrange-type experiment with measurement sites located upwind and downwind of an orographic cloud as well as within the cloud, enabled investigation of changes in the physicochemical properties of an air mass as it underwent cloud processing. Sulfur isotope abundances were measured in gas-phase SO₂

and particulate sulfate during three cloud events: FCE 7.1, 11.2, and 11.3 (described in text S1 and table S2).

The effect of cloud processing on the particle population and the magnitude of aerosol radiative forcing critically depends on the pathway responsible (e.g., in situ oxidation, H₂SO₄ condensation) for in-cloud sulfate production. Generally, H₂O₂ is consumed early in a cloud's lifetime; thus, most of the sulfate produced from aqueous SO₂ oxidation by H₂O₂ is added to the most cloud condensation nuclei (CCN)-active particles (7), where it has a negligible effect on downwind CCN number concentration and aerosol radiative forcing. Oxidation by O₃ in cloud droplets is very slow at low pH (<5.5) and represents only a small proportion of global in-cloud SO₂ oxidation (8, 9). The climatic effect of sulfate produced from transition metal ion (TMI)-catalyzed oxidation depends on the source of the TMIs: Sulfate produced from oxidation catalyzed by TMIs in fine particles can greatly alter downwind CCN properties and radiative forcing, whereas sulfate produced by TMIs in coarse particles will result in a weaker radiative forcing. Understanding and accurately modeling partitioning between the major oxidation pathways is critical to predict the magnitude and spatial distribution of sulfate aerosol cooling in assessments of future climate.

H₂O₂ is thought to be the major in-cloud SO₂ oxidant (5, 10, 11): Four of the 12 models used in the IPCC Fourth Assessment Report and/or

the AeroCom global intercomparison exercise consider H₂O₂ to be the only aqueous-phase oxidant for SO₂ (table S1). Models including only H₂O₂ and O₃ as in-cloud oxidants attribute 64 to 83% of global sulfate production to aqueous-phase chemistry and 17 to 36% to gas-phase oxidation. They underpredict the observed sulfate concentration by ~20% and overestimate SO₂ concentrations by ~50%, which suggests that a major oxidation pathway is missing or underestimated (12–16). The rate of the TMI-catalyzed oxidation of SO₂ by oxygen is poorly characterized because of the complex interactions among different TMIs (17, 18). Δ¹⁷O results (19) showed that the contribution of TMI catalysis to sulfate production was strongly underestimated. However, the inclusion of SO₂ oxidation catalyzed by anthropogenic TMIs into the modeled sulfur cycle (GEOS-Chem) has not been able to resolve the discrepancy between modeled and measured SO₂ and sulfate concentrations (20): SO₂ concentrations in the global EMEP domain are overestimated by a factor of 1.8 to 2.7 and sulfate concentrations by a factor of 1.5 to 3.7 for simulations including TMI chemistry; for simulations without TMI chemistry, these same concentrations are overestimated by a factor of 1.9 to 3.0 and by a factor of 0.8, respectively.

Stable sulfur isotopes show distinctive fractionation during chemical reactions and are therefore useful for investigating the in-cloud sulfur cycle. Oxidation by H₂O₂ and O₃ produces sulfate that is enriched in ³⁴S [+15.1 to +19.9 per mil (‰) depending on pH] relative to the reactant SO₂, whereas oxidation by TMI catalysis produces sulfate depleted in ³⁴S (−9.5 ± 3.1‰) relative to SO₂ (21–23). The change in isotopic composition of SO₂ gas between the upwind and downwind stations was used to calculate the fractionation factor for the cloud, α_{cloud} (text S2 and table S3), which was compared with fractionation factors for known reactions to determine the dominant SO₂ oxidation pathway occurring in the cloud (Table 1). The α_{cloud} values clearly show that H₂O₂ or O₃ dominates in-cloud oxidation only during the first nighttime event; during the second nighttime and the daytime event, TMI catalysis is the dominant oxidation pathway. The cloud water pH values were low (fig. S2); thus, oxidation shown isotopically to be due to H₂O₂ or O₃ will be dominated by H₂O₂ and is hereafter referred to as oxidation by H₂O₂. Both the TMI and H₂O₂ concentrations in cloud water at HCCT were within normal ranges during all three

¹Particle Chemistry Department, Max Planck Institute for Chemistry, D-55128 Mainz, Germany. ²Department of Earth Sciences, IISER Mohali, Sector 81 SAS Nagar, Manauli P.O. 140306, India. ³Leibniz Institute for Tropospheric Research (TROPOS), 04318 Leipzig, Germany. ⁴Department of Atmospheric Science, Colorado State University, Fort Collins, CO 80523, USA. ⁵Earth System Science Research Centre, Institute for Geosciences, University of Mainz, D-55128 Mainz, Germany. ⁶Institute for Atmospheric Physics, University of Mainz, D-55128 Mainz, Germany.

*Corresponding author. E-mail: elizah@mit.edu (E.H.); baerbel.sinha@mpic.de (B.S.)

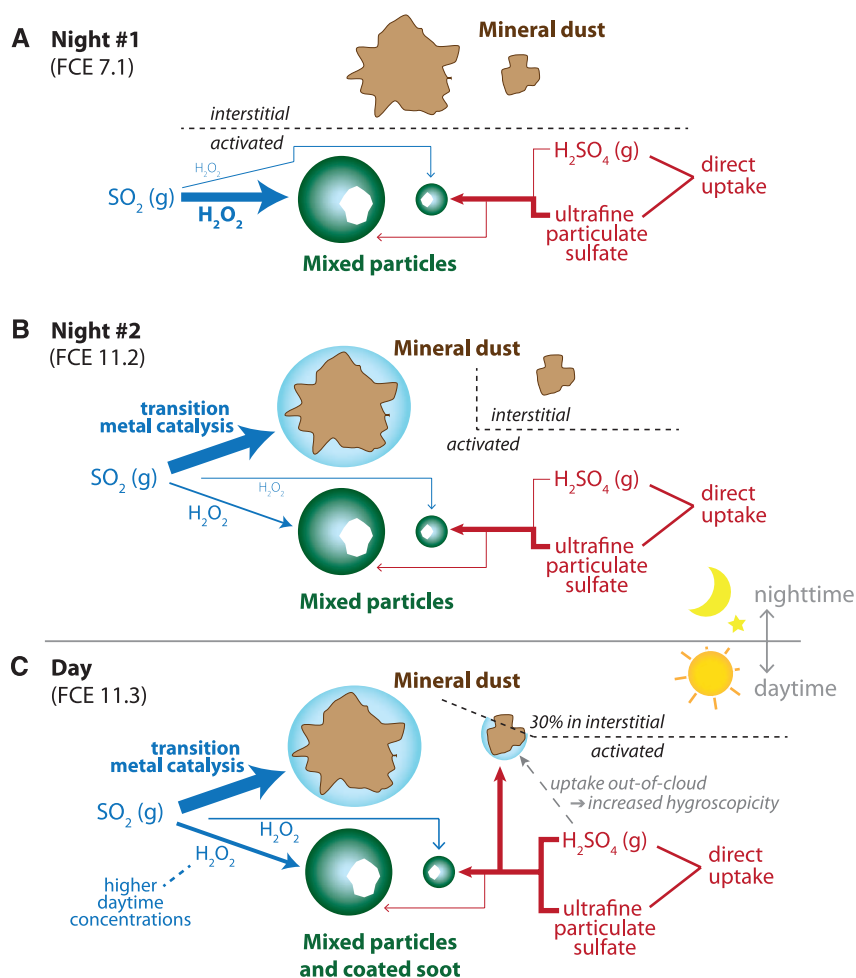
†Present address: Earth, Atmospheric and Planetary Sciences, Massachusetts Institute of Technology, Cambridge, MA 02142, USA.

‡Present address: Department of Earth and Planetary Sciences, ARC Centre for Core to Crust Fluid Systems, Building E7A, Macquarie University, North Ryde, NSW 2109, Australia.

Table 1. Dominant in-cloud SO₂ oxidation pathway determined from the fractionation of sulfur isotopes. Official event names are shown in brackets. α_{cloud} is the fractionation factor for SO₂ removal in the cloud. Oxidant refers to the oxidation reaction that agrees with the observed in-cloud isotope fractionation; α_{ox} is the corresponding known, laboratory-derived fractionation factor (21).

Event	LWC (g m ⁻³)	α _{cloud} (‰)	Oxidant	α _{ox} (‰)
Night 1 (FCE 7.1)	0.14	11.6 ± 9.8	H ₂ O ₂	15.1 ± 1.3
Night 2 (FCE 11.2)	0.37	−16.1 ± 9.5	TMI catalysis	−9.5 ± 3.1
Day (FCE 11.3)	0.32	−10.8 ± 4.9	TMI catalysis	−9.5 ± 3.1

Fig. 1. Summary of the sulfur cycle occurring in clouds during three measurement periods of the HCCT-2010 campaign. (A and B) The first and second nighttime events, FCE 7.1 and FCE 11.2; **(C)** the daytime event, FCE 11.3. Processes occurring only on particles that activated to form cloud droplets are shown on the “activated” side of the dashed lines. The proportion of activated particles in each class was determined from NanoSIMS (nano-secondary ion mass spectrometry) isotopic mass balance, under the assumption that the droplet residue and interstitial dust remix to form the downwind dust sample (see also table S7). The thickness of the arrow qualitatively represents the relative strength of the flux.



events (7, 24–27) (table S2 and figs. S2 and S3). The dominance of TMI-catalyzed oxidation could therefore be a widespread phenomenon, as suggested previously (19, 20).

Isotopic analysis of single particles, in combination with isotopic measurements of gas-phase sulfur, allowed the major sulfate addition pathways to be resolved for particle class (text S2 and tables S4 and S5). The major sulfate sources to particles are summarized in Fig. 1. Sulfate from H₂O₂ oxidation and direct uptake of H₂SO₄ gas and ultrafine particulate are the two dominant sources of sulfate for activated mixed particles (containing a mixture of secondary organic aerosol (SOA) and secondary inorganic aerosol (SIA; Fig. 2, A and B) and activated fine-mode mineral dust particulate. The oxidation source is more important for larger particles (>600 nm; text S1), whereas direct uptake dominates sulfate addition to smaller particles (<600 nm).

The distinctive fractionation during TMI-catalyzed oxidation showed that it was the dominant sulfate source only for coarse mineral dust (Fig. 2, E and F, >900 nm). Mineral dust represented <1% of the CCN number concentration (table S7); thus, oxidation in cloud droplets nucleated on mineral dust must be extremely fast

to compete with other oxidation pathways and dominate SO₂ removal. Previous results have suggested that anthropogenic TMIs are an important catalyst for SO₂ oxidation in Europe, whereas the low solubility of natural TMIs means that they will be unimportant as catalysts (20). Our results show, however, that natural TMIs catalyzed the dominant oxidation pathway. A recent laboratory study showed that significant amounts of TMIs are leached from natural dust and can rapidly oxidize SO₂ in the aqueous phase (22). The solubility of TMIs in dust may be increased through aging and uptake of acidic compounds such as sulfuric and nitric acid. Anthropogenic TMIs are expected to be concentrated on fine-mode combustion particles, whereas natural TMIs lead to sulfate production in the coarse mode; thus, the radiative forcing potential of the sulfate produced from TMI-catalyzed oxidation by natural TMIs will be much lower than that of sulfate produced by anthropogenic TMIs.

Conditions during the three events were examined to explain why H₂O₂ was the dominant oxidant only during the first nighttime event. The only major difference among the three events is the liquid water content (LWC) (0.14, 0.37, and 0.32 g m⁻³ during the first and second

nighttime events and the daytime event, respectively; see text S2 and table S2). The total concentration of TMIs was similar in all three events; however, differences in the TMI profiles for the three events (fig. S3) suggest that during the first nighttime event, coarse mineral dust was not the major source of TMIs to the cloud water, allowing H₂O₂ oxidation to dominate. Particle size distributions and other results confirm that coarse mineral dust was present in the particle population during the first nighttime event but was unable to activate (text S2 and fig. S4). Our results show that although TMIs are present at HCCT from both anthropogenic and natural sources, the natural mix of TMIs leads to stronger synergistic interactions and faster SO₂ oxidation, and therefore dominates in situ sulfate production.

Comparing the isotopic observations with theoretical calculations for in-cloud SO₂ oxidation during HCCT confirms that the rate of TMI catalysis used in current models results in a strong underestimation of the pathway's importance (text S2). A reaction rate constant for TMI-catalyzed oxidation of S(IV) that considers synergistic effects of different TMIs is available only for the most widely studied system of Fe(III) and Mn(II) (28). Estimations using this rate constant (fig. S5A)

Fig. 2. Characteristic particle types collected during the HCCT-2010 campaign. Images are scanning electron micrographs of filter samples. (A) Accumulation-mode mixed SOA-SIA droplet. (B) Coarse-mode mixed SOA-SIA droplet. (C and D) Soot particles, without (C) and with (D) organic coating. (E and F) Mineral dust particles, without (E) and with (F) organic coating. SOA particles and organic coatings appear dark gray, filter pores appear black, and filter material appears gray. Scale bars, 200 nm [(A), (C), (D)], 1000 nm [(B), (E), (F)].

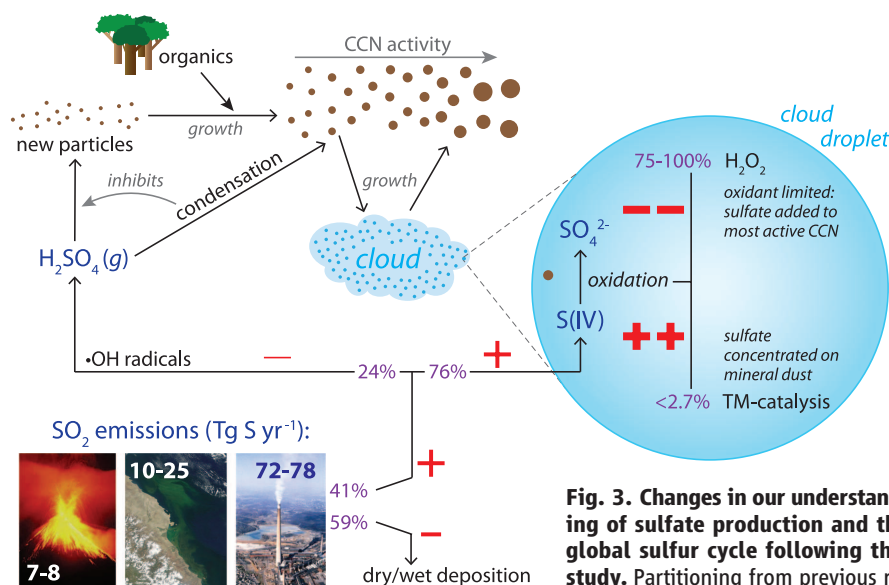
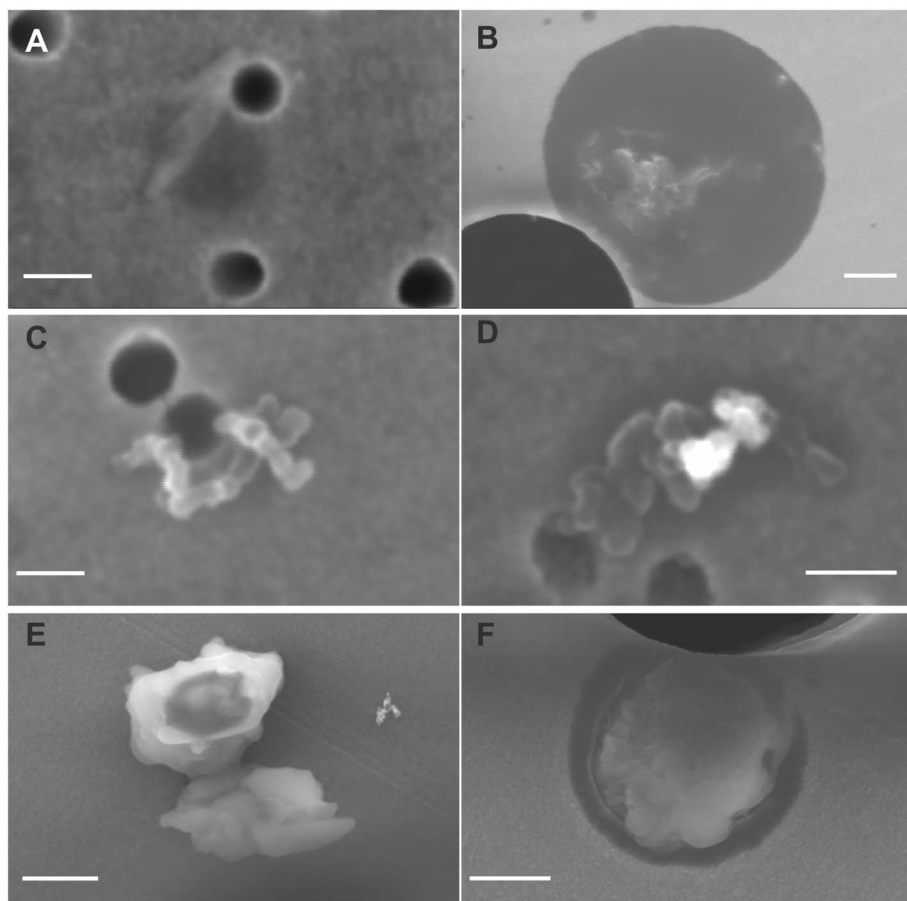


Fig. 3. Changes in our understanding of sulfate production and the global sulfur cycle following this study. Partitioning from previous results (purple) are averages from the

models in table S1. Red plus and minus symbols show how the current study changes our understanding of the sulfur cycle; the number and size of plus and minus symbols represent the expected magnitude of the change and our confidence in it, respectively.

attribute only a few percent of sulfate production to the TMI catalysis pathway. The results of theoretical calculations considering possible interactions of the whole range of measured soluble

TMIs (fig. S5B) show much better agreement with the isotopic measurements.

Because the total TMI concentrations are similar for all three events, the different oxidation

regimes indicated by the S-isotope measurements show that not all metals are equally active in catalyzing oxidation. For example, FCE 7.1 had relatively high Ni^{2+} , Zn^{2+} , and Cu^{2+} concentrations but displayed low TMI-catalyzed oxidation, which suggests that these metals are less active in oxidation, in agreement with laboratory studies (29, 30). Ti is a strong SO_2 oxidant on dust surfaces and could play an important role in catalytic activity. Observations indicate that Ti is leached from natural dust with an efficiency equal to that of Fe (22). The Ti/Fe ratio in upwind particles was higher in FCE 11.2 and 11.3 (average Ti/Fe of 0.05 and 0.03, respectively, versus an average of 0.02 for FCE 7.1). It is possible that the higher Ti/Fe ratio plays a role in the very high reaction rate for TMI-catalyzed oxidation during FCE 11.2 and 11.3.

Reactive uptake coefficients (γ_{obs}) for oxidation of SO_2 by TMI catalysis (text S2 and table S9) can be compared with the sulfur cycle in current models to provide an estimate of how strongly the pathway is underestimated on a global scale. The values of γ_{obs} for mineral dust during FCE 11.2 and 11.3 ($\gamma_{\text{obs}} = 0.03$ to 0.10) are several orders of magnitude higher than the γ value of 10^{-4} used for oxidation of SO_2 on the surface of mineral dust in the ECHAM-HAMMOZ model (31). OsloCTM2 was the only model found that explicitly includes the TMI catalysis pathway

(14); however, the defined maximum modeled rate of $5.56 \times 10^{-6} \text{ s}^{-1}$ is slower than observed during HCCT by one to two orders of magnitude. On the basis of $\Delta^{17}\text{O}$ results, Alexander *et al.* (20) predicted that TMI catalysis contributes 9 to 17% of global sulfate production. Comparison of fractionation factors with previously measured $\delta^{34}\text{S}$ values of SO_2 and sulfate (text S2 and table S10) enables us to predict that the contribution of TMI catalysis to sulfate production varies between 1% (urban) and 58% (rural) at continental sites; it is likely to dominate SO_2 oxidation in all clouds with sufficient supersaturation to activate mineral dust (as summarized in Fig. 3). The results of Alexander *et al.* (20) and Sofen *et al.* (32) suggest that increasing TMI-catalyzed oxidation primarily reduces estimated oxidation by the other aqueous pathways and has little effect on the proportion of SO_2 oxidized in the gas phase, whereas Goto *et al.* (6) found that treatment of aqueous-phase sulfur chemistry in models had the largest impact on sulfate distribution of the parameters tested.

Characterizing the rate of TMI catalysis and including it in models will improve agreement between modeled and observed SO_2 concentrations. The inclusion of the TMI catalysis pathway into GEOS-Chem (20) showed the potential importance of TMI-catalyzed oxidation attributed to anthropogenic TMIs; however, comparisons of models and observations showed a strong overestimation of both SO_2 and sulfate concentrations (12–16). Our observations showed that sulfate produced by TMI catalysis is dominated by natural TMIs and concentrated on coarse mineral dust. It will be removed from the atmosphere relatively quickly, improving agreement between models and observations; it will also result in a minimal modification of the aerosol size distribution and reduced estimates of indirect and direct forcing associated with sulfate from in-cloud oxidation. The estimated level of sulfate aerosol cooling will therefore be much lower and will show a strongly altered spatial distribution, which will have important consequences for assessments of anthropogenic climate change (1). The sulfate produced will also acidify the dust, with important consequences for iron solubility and bioavailability (33). In the coming decades, SO_2 emissions are expected to increase in India and China (34). Windblown dust emissions in both these countries are high; thus, future aerosol cooling may be strongly overpredicted by current climate chemistry models. The results from HCCT provide a size- and particle type-dependent view of in-cloud oxidation that will improve agreement between models and observations and will affect predictions of radiative forcing associated with sulfate in future decades.

References and Notes

1. M. O. Andreae, C. D. Jones, P. M. Cox, *Nature* **435**, 1187 (2005).
2. M. Kulmala, U. Pirjola, J. M. Makela, *Nature* **404**, 66 (2000).
3. S. Solomon *et al.*, in *Climate Change 2007: The Physical Science Basis. Contribution of Working Group I to the*

- Fourth Assessment Report of the Intergovernmental Panel on Climate Change*, S. Solomon *et al.*, Eds. (Cambridge Univ. Press, New York, 2007), technical summary.
4. J. Langner, H. Rodhe, P. J. Crutzen, P. Zimmermann, *Nature* **359**, 712 (1992).
 5. S. Mertes *et al.*, *Atmos. Environ.* **39**, 4233 (2005).
 6. D. Goto, T. Nakajima, T. Takemura, K. Sudo, *Atmos. Chem. Phys.* **11**, 10889 (2011).
 7. K. N. Bower *et al.*, *Atmos. Environ.* **31**, 2527 (1997).
 8. C. F. Botha, J. Hahn, J. J. Pienaar, R. Vaneldik, *Atmos. Environ.* **28**, 3207 (1994).
 9. M. Chin *et al.*, *J. Geophys. Res.* **101**, 18667 (1996).
 10. G. P. Gervat *et al.*, *Nature* **333**, 241 (1988).
 11. D. A. Hegg, R. Majeed, P. F. Yuen, M. B. Baker, T. V. Larson, *Geophys. Res. Lett.* **23**, 2613 (1996).
 12. L. A. Barrie *et al.*, *Tellus* **53B**, 615 (2001).
 13. L. Rotsteyn, U. Lohmann, *J. Geophys. Res.* **107**, 4592 (2002).
 14. T. Berghen, T. Berntsen, I. Isaksen, J. Sundet, *J. Geophys. Res.* **109**, D19310 (2004).
 15. D. A. Hegg, D. S. Covert, H. Jonsson, D. Khelif, C. A. Friehe, *Tellus* **56B**, 285 (2004).
 16. A. L. Redington, R. G. Derwent, C. S. Witham, A. J. Manning, *Atmos. Environ.* **43**, 3227 (2009).
 17. J. Tilly, M. Lewicki, Z. Tomaszewski, J. Toczkowski, *J. Chem. Technol. Biotechnol.* **52**, 301 (1991).
 18. A. Rani, D. S. N. Prasad, P. V. S. Madnawat, K. S. Gupta, *Atmos. Environ.* **26A**, 667 (1992).
 19. J. R. McCabe, J. Savarino, B. Alexander, S. L. Gong, M. H. Thiemens, *Geophys. Res. Lett.* **33**, L05810 (2006).
 20. B. Alexander, R. J. Park, D. J. Jacob, S. L. Gong, *J. Geophys. Res.* **114**, D02309 (2009).
 21. E. Harris *et al.*, *Atmos. Chem. Phys.* **12**, 407 (2012).
 22. E. Harris *et al.*, *Atmos. Chem. Phys.* **12**, 4867 (2012).
 23. E. Harris, B. Sinha, P. Hoppe, S. Foley, S. Borrmann, *Atmos. Chem. Phys.* **12**, 4619 (2012).
 24. D. L. Sedlak *et al.*, *Atmos. Environ.* **31**, 2515 (1997).
 25. P. Laj *et al.*, *Atmos. Environ.* **31**, 2589 (1997).

26. P. Laj *et al.*, *Atmos. Environ.* **31**, 2503 (1997).
27. K. Plessow, K. Acker, H. Heinrichs, D. Möller, *Atmos. Environ.* **35**, 367 (2001).
28. T. Ibusuki, K. Takeuchi, *Atmos. Environ.* **21**, 1555 (1987).
29. T. E. Graedel, M. L. Mandich, C. J. Weschler, *J. Geophys. Res.* **91**, 5205 (1986).
30. I. Grgić, V. Hudnik, M. Bizjak, J. Levec, *Atmos. Environ.* **25**, 1591 (1991).
31. L. Pozzoli *et al.*, *J. Geophys. Res.* **113**, D07308 (2008).
32. E. Sofen, B. Alexander, S. A. Kunasek, *Atmos. Chem. Phys.* **11**, 3565 (2011).
33. T. D. Jickells *et al.*, *Science* **308**, 67 (2005).
34. S. Solomon *et al.*, Eds., *Climate Change 2007: The Physical Science Basis. Contribution of Working Group I to the Fourth Assessment Report of the Intergovernmental Panel on Climate Change* (Cambridge Univ. Press, New York, 2007).

Acknowledgments: We thank E. Gröner for his support with the NanoSIMS analyses, J. Huth for his help with the scanning electron microscopy and energy-dispersive x-ray spectroscopy analyses, and all the participants of HCCT-2010 for an interesting and successful campaign. This research was funded by the Max Planck Society and the Max Planck Graduate Centre. The HCCT-2010 campaign was partially funded by the Deutsche Forschungsgemeinschaft under contract HE 3086/15-1. Participation of Colorado State University scientists was supported by grants from TROPOS Leipzig and by NSF grant AGS 1050052.

Supplementary Materials

www.sciencemag.org/cgi/content/full/340/6133/727/DC1
 Texts S1 and S2
 Figs. S1 to S5
 Tables S1 to S10
 References (35–89)

1 October 2012; accepted 28 February 2013
 10.1126/science.1230911

Networks of bZIP Protein-Protein Interactions Diversified Over a Billion Years of Evolution

Aaron W. Reinke, Jiyeon Baek, Orr Ashenberg, Amy E. Keating*

Differences in biomolecular sequence and function underlie dramatic ranges of appearance and behavior among species. We studied the basic region-leucine zipper (bZIP) transcription factors and quantified bZIP dimerization networks for five metazoan and two single-cell species, measuring interactions in vitro for 2891 protein pairs. Metazoans have a higher proportion of heteromeric bZIP interactions and more network complexity than the single-cell species. The metazoan bZIP interactomes have broadly similar structures, but there has been extensive rewiring of connections compared to the last common ancestor, and each species network is highly distinct. Many metazoan bZIP orthologs and paralogs have strikingly different interaction specificities, and some differences arise from minor sequence changes. Our data show that a shifting landscape of biochemical functions related to signaling and gene expression contributes to species diversity.

Differences in transcriptional regulation between species contribute to developmental and functional outcomes (1). Both changes in cis regulatory elements and coding mutations in transcription factors affecting protein-DNA and protein-protein interactions can influence gene regulation (2–5). The basic leucine-zipper

(bZIP) proteins, a large class of multifunctional transcription factors, provide an opportunity to study the evolution of biomolecular interactions. bZIPs can be identified in eukaryotic genomes by a basic DNA binding region followed by a leucine-zipper coiled-coil motif. bZIP proteins can form homodimers and heterodimers via the coiled-coil region, and the dimer that forms influences the DNA sites that can be bound (6). Because bZIP proteins interact with other bZIPs, it is possible to compile a comprehensive list of candidate

Massachusetts Institute of Technology, Department of Biology, Cambridge, MA 02139, USA.

*Corresponding author. E-mail: keating@mit.edu